

Development and Optimization of UV-Induced Chemical Foaming Process

Podchara Rattanakawin, Kai Yamamura,
Kenji Yoshimoto*, and Masahiro Ohshima**

*Department of Chemical Engineering, Kyoto University,
Katsura, Nishikyo-ku, Kyoto 615-8510, Japan*

**yoshimoto1@cheme.kyoto-u.ac.jp*

***ohshima.masahiro.2w@kyoto-u.ac.jp*

In this study, we have investigated a UV-induced chemical foaming method to create a nanocellular polymer thin film. A small amount of photoacid generator (PAG) was mixed with poly(methyl methacrylate-*co-tert*-butyl acrylate) (PMMA-*co*-PtBA). After UV irradiation followed by heating, *tert*-butyl ester group in the PtBA was deprotected with the acid generated from the PAG, and isobutene gas was produced in the polymer matrix. The resulting polymer foamed with the gas had cell size and cell density ranging from 100 to 200 nm and from 1×10^{13} to 9×10^{13} cells/cm³, respectively. Several key parameters were found that would affect largely on the formation of the nanocellular structure, i.e., foaming time and temperature, UV dose, molecular weight of polymer.

Keywords: Chemical foaming, Polymer film, Nanocellular foam

1. Introduction

Nanocellular foams, defined as polymer foams with cell size less than 1000 nm have received a large attention for their superior thermal and mechanical properties [1-3]. Due to Knudsen effect, the thermal conductivity of the nanocellular foams significantly decreases by reducing the cell size less than the mean free path of air (~100 nm) [4,5]. In addition, the highly dense, nano-size pores may interfere with the crack propagation. This results in an improvement of the mechanical properties, such as the Young's modulus and impact resistance [6,7].

Currently, most of the researches in nanocellular foams are conducted by physical foaming, where an inert gas, such as CO₂ or N₂, is introduced into the polymer matrix at high pressure [8]. The cell size and density can be controlled by adjusting the pressure drop rate during the bubble nucleation [9], inducing heterogeneous nucleation with bubble nucleating agents [10,11], and using block copolymer templates with different gas absorption in each block [12,13]. These methods enable to fabricate highly dense cells in nanometer size. However, the major disadvantage of physical foaming is the complexity of the process, requiring

high pressure and temperature.

Chemical foaming is another well-known foaming process where a chemical blowing agent is mixed into the polymer matrix. Upon heating at a high temperature, the chemical blowing agent is thermally decomposed and the gas is produced to generate the cells. The cell structure is predetermined by the size and dispersion of chemical blowing agents. In the conventional chemical foaming, the chemical blowing agents have a micrometer size with a limited dispersivity [14,15]; it is not directly applicable to nanocellular foaming.

To overcome such limitations, Kojima et al. demonstrated the new chemical process in which the polymer itself act as the chemical blowing agent [16] (Fig. 1). Poly(methyl methacrylate-*co-tert*-butyl acrylate) (PMMA-*co*-PtBA) was selected as a self-formable polymer matrix and mixed with a small amount of the photoacid generator (PAG). By irradiating the sample with UV light, an acid was generated from the PAG. Upon heating, the acid diffused around and deprotected *tert*-butyl ester in PtBA (Fig. 2). Consequently, isobutene gas was produced to foam the polymer. Kojima et al.

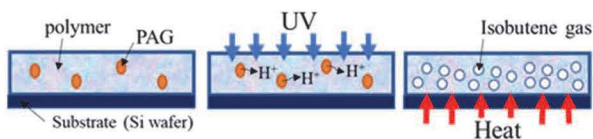


Fig. 1. Schematic flow of UV-induced chemical foaming process [16].

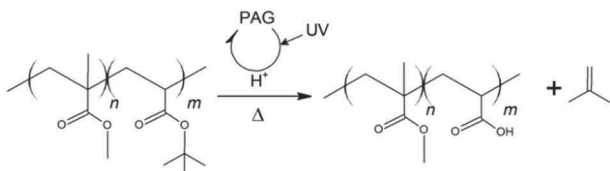


Fig. 2. Deprotection reaction of *tert*-butyl ester in PMMA-*co*-PtBA [16].

successfully created polymer foams with cell size of 220-400 nm [16]. However, the fundamental mechanisms of the UV-induced chemical foaming process have not yet been elucidated. Therefore, in this study, we investigated how the nanocellular structure would be generated in the UV-induced chemical foaming by varying the process conditions and materials parameters, such as amount of UV irradiation, weight fraction of PAG, foaming time and temperature, and polymer's molecular weight.

2. Experimental

A random copolymer, PMMA-*co*-PtBA (Polymer Source Inc.) was used as a foamable polymer with the specifications shown in Table 1. Three PMMA-*co*-PtBA samples were used here, which have similar mole fraction of PtBA (f_{PtBA}) with largely different weight-averaged molecular weights (M_w). Since the PtBA is set to be the major component, the glass transition temperature of the PMMA-*co*-PtBA (T_g) becomes closer to that of pure PtBA, 41 °C. For the majority of the experiments, PMMA-*co*-PtBA with the M_w of 258000 was used.

Table 1. PMMA-*co*-PtBA specifications.

No.	f_{PtBA}	M_w	PDI	T_g (°C)
1	0.75	258000	1.28	45
2	0.64	108500	1.13	53
3	0.72	44000	1.20	57

For PAG, an iodonium salt photoacid generator, BBI-109 (Midori Kagaku) was selected since the maximum absorption wavelength was 238 nm, close to the wavelength of our UV lamp, 254 nm.

PMMA-*co*-PtBA thin films were prepared by solution casting. A polymer solution was prepared by dissolving 5.00 wt% of PMMA-*co*-PtBA and

0.25 wt% of BBI-109 into propylene glycol methyl ether acetate (PGMEA) (Sigma Aldrich). All chemicals were used as received from the supplier. As soon as 20 μ L of the solution was casted on a 1 cm \times 1 cm silicon wafer, the film was covered with aluminum foil to prevent the activation of BBI-109 and dried at room temperature overnight. The film was further dried on a hot plate at 100 °C for 5 minutes to ensure no residual solvent. After all the drying steps, the colorless transparent PMMA-*co*-PtBA films were irradiated using a 254 nm UV lamp (UVGL-58, UVP) with intensity of \sim 1 mW/cm². Immediately after the UV irradiation, the polymer film was heated on a hotplate. During the heating, the isobutene gas was produced by the acid diffusion, and the nanocellular structure was generated. In what follows, the heating time and temperature are referred to as foaming time and temperature, respectively.

The resulting cell structure was observed by scanning electron microscope (SEM) (SU8000, Hitachi High-Tech). First, the foamed film was cracked along with the silicon substrate. Then, approximately 1-nm-thick Pt was deposited on the cross-section of the foamed film, prior to the observation by SEM.

The rheological properties of PMMA-*co*-PtBA was measured using a rheometer (ARES, TA Instrument). PMMA-*co*-PtBA bulk sample with dimension of 40 mm \times 10 mm \times 1 mm was prepared by compression molding at 150 °C and \sim 20-30 MPa. In the torsion-mode experiments, complex viscosity of the sample, η^* was measured under the maximum strain of 1% and frequency of 0.63 rad/s.

3. Results and discussion

3.1. Formation of nanocellular structure

The following conditions were used as a standard case to demonstrate the formation of the nanocellular structure. The M_w of PMMA-*co*-PtBA was fixed at 258000. The film thickness after the drying step was \sim 10 μ m estimated from the cross-section SEM image [Fig. 3(a)]. Excess UV dosage of 3600 J/cm² was used to ensure that activation of the PAG was completed. By heating the film on a hotplate at 80 °C for 180 s, a foamed film was obtained. The cross-section SEM image of the foamed film was shown in Fig. 3(b). Figure 3(c) shows the cross-section SEM image near the center of the foamed film [Fig. 3(b)] with a higher magnification. The cell structure was analyzed from Fig. 3(c) using the procedure described in Ref. [17]. The cell size (d) and density (N) were calculated

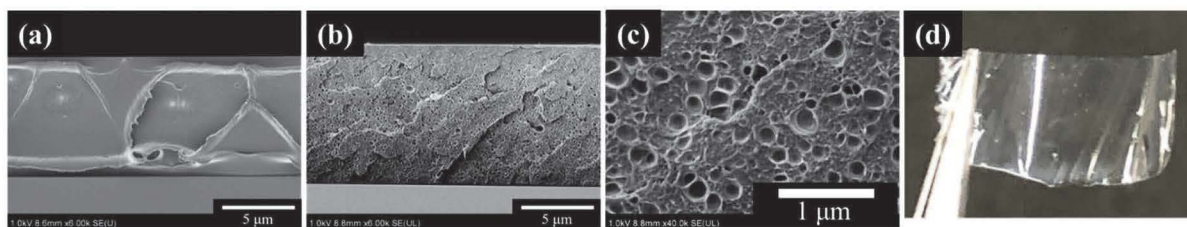


Fig. 3. Cross-section SEM images of PMMA-co-PtBA film: (a) as casted, (b, c) foamed at 80 °C for 180 s with low and high magnification, respectively. (d) Optical image of the PMMA-co-PtBA film peeled off from the Si substrate, after foaming at 80 °C for 180 s.

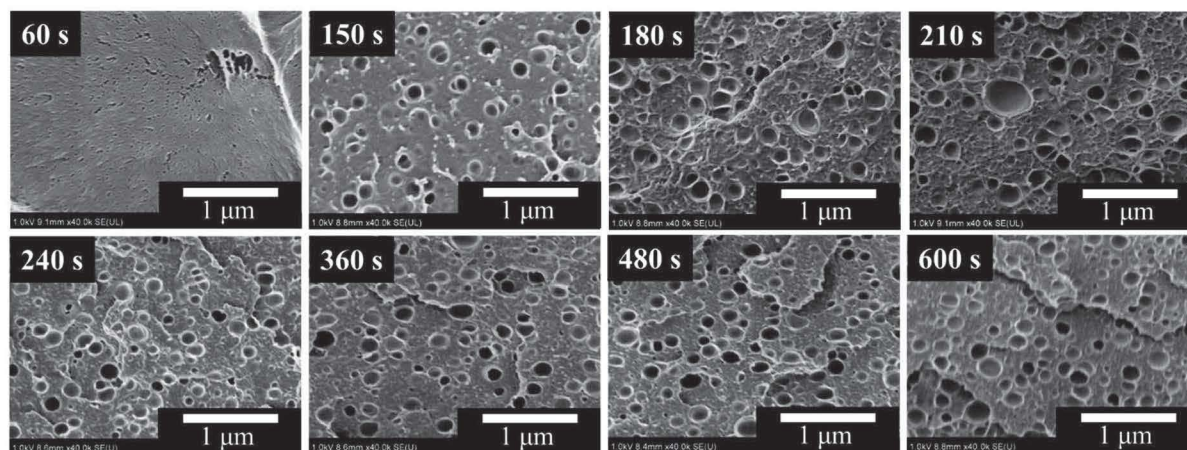


Fig. 4. Cross-section SEM images of PMMA-co-PtBA films foamed at 80 °C. The number on the top right corner corresponds to the foaming time.

from

$$d = \Sigma d_i/n, \quad N = (n/A)^{3/2}, \quad (1)$$

where d_i , n and A are the circle-equivalent diameter of individual cell, the total number of cells, and the area of the cross-section SEM image. Using Eq. (1), cell size and density of the foamed sample in Fig. 3(c) were estimated at 139 ± 40 nm and 4.7×10^{13} cells/cm³. These numbers are close to those obtained by Kojima et al. [16], demonstrating that our UV-induce chemical foaming process worked properly.

3.2. Foaming time and temperature

First, effect of foaming time was investigated. The experiments were conducted using the same materials and conditions as those described in the previous section, except the foaming time. Figure 4 illustrates the cross-section SEM images of the film heated at 80 °C for 60 to 600 s. The cell size and density estimated from the SEM images were plotted in Fig. 5 as a function of foaming time.

Although no cells were observed at the foaming time of 60 s, cells were sparsely formed at 150 s. This indicates that the *tert*-butyl ester deprotection reaction started sometime in between 60 and 150 s. As the foaming time was increased from 150 to 210

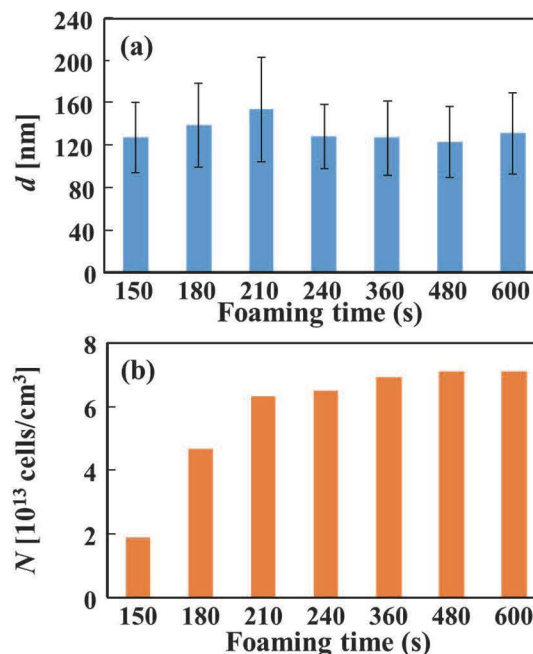


Fig. 5. Change in cell structure with foaming time: (a) cell size (d) and (b) cell density (N). Both were estimated from the SEM images in Fig. 4.

s, the cell size and the density were gradually increased from 128 to 154 nm [Fig. 5(a)] and from 1.8×10^{13} to 6.3×10^{13} cells/cm³ [Fig. 5(b)], respectively. It is most likely that during 150 and

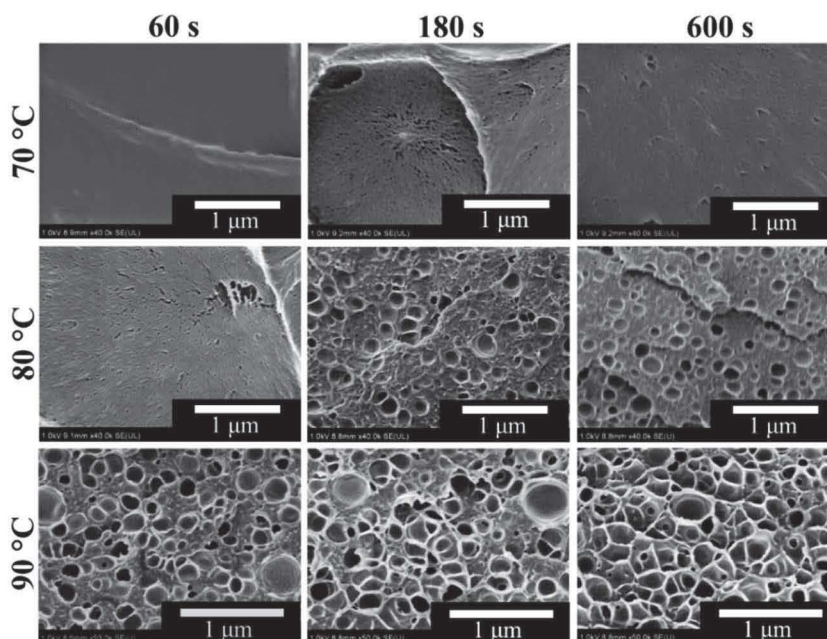


Fig. 6. Cross-section SEM images of PMMA-*co*-PtBA films foamed at different temperatures: (top) 70 °C, (middle) 80 °C and (bottom) 90 °C. At each foaming temperature, the SEM images were taken at the foaming time of (left) 60s, (center) 180 s, (right) 600 s.

210 s, more isobutene gas was produced from the *tert*-butyl ester deprotection reaction by the acceleration of acid diffusion. Interestingly, a slight decrease in cell size was observed from 240 to 360 s [Fig. 5(a)]. It is speculated that most of the *tert*-butyl ester group in PtBA was deprotected by 240 s, and then that excess amount of the isobutene gas was diffused out of the polymer matrix. After 360 s, the cell structure was almost unchanged.

Next, the foaming temperature was varied while keeping the other conditions the same. Three foaming temperatures were investigated: 70, 80 and 90 °C. At each temperature, the cross-section SEM images of the films were taken after heating for 60, 180 and 600 s (Fig. 6). At 70 °C, no cells were observed within 600 s of foaming. This signifies that 70 °C was too low to initiate the *tert*-butyl ester decomposition reaction. In contrast to 70 °C, large cells were formed throughout the image after heating the film at 80 °C for 180 s or 90 °C for 60 s. The cell size and the cell density of the foamed films for 600 s are summarized in Table 2. The size and the density at 90 °C are found to be larger by ~54 nm and ~1.7×10¹² cells/cm², respectively, than those at 80 °C. Such increase may be explained by the softening of polymer matrix at higher temperature. As shown in Fig. 7, the complex viscosity of the bulk PMMA-*co*-PtBA, η^* decreases monotonically with temperature. Indeed, η^* decreases from 9.1 × 10⁹ to 6.4 × 10⁵ Pa·s when the foaming temperature increases from 80 to 90 °C. Note that the η^* was

Table 2. Cell size and density after foaming for 600 s.

Foaming Temp. (°C)	Cell Size (nm)	Cell Density (cells/cm ³)
80	131 ± 39	7.1 × 10 ¹³
90	185 ± 45	8.8 × 10 ¹³

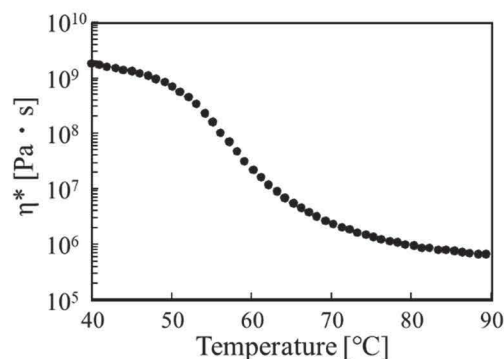


Fig. 7. Changes of the complex viscosity of the bulk PMMA-*co*-PtBA (η^*) with temperature.

measured using the bulk PMMA-*co*-PtBA without PAG. Since the PMMA-*co*-PtBA loses the weight during the foaming process, η^* would be even smaller, enhancing the foaming at higher temperature.

3.3. UV irradiation

The UV dose was varied to 60, 180, 300 and 600 mJ/cm², while the other parameters are kept the same as the standard case. The cross-section SEM images are summarized in Fig. 8, and the cell size

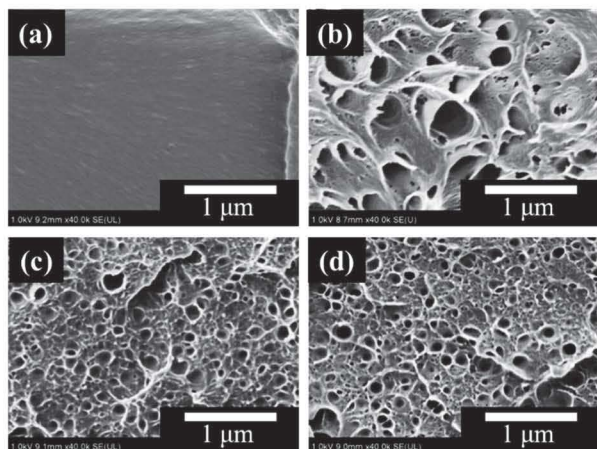


Fig. 8. Cross-section SEM images of PMMA-co-PtBA films irradiated with UV dose of (a) 60, (b) 180, (c) 300 and (d) 600 mJ/cm² and foamed at 80 °C for 180 s.

Table 3. Effect of UV dose on cell structure.

UV Dose (mJ/cm ²)	Cell Size (nm)	Cell Density (cells/cm ³)
180	323 ± 132	0.7 × 10 ¹³
300	140 ± 33	4.6 × 10 ¹³
600	141 ± 33	5.0 × 10 ¹³

and the cell density of each SEM image are listed in Table 3. No foaming was observed in 60 mJ/cm² irradiated film. With 180 mJ/cm² irradiation, the cells were sparsely distributed with a relatively large size, indicating that the activation of PAG was insufficient and the gas was generated locally. As the UV dose was increased to 300 mJ/cm², smaller cells were formed with a higher density. Since the cell size and the cell density remained almost the same between 300 mJ/cm² and 600 mJ/cm², it is most likely that the PAG was fully activated with 300 mJ/cm².

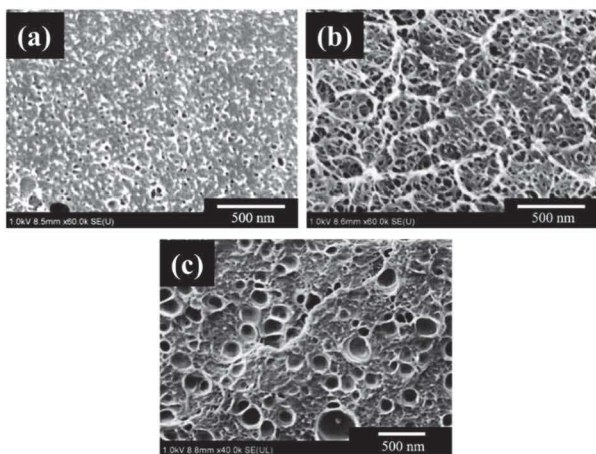


Fig. 9. Cross-section SEM images of PMMA-co-PtBA films with M_w of (a) 44000, (b) 108500 and 258000, foamed at 80 °C for 180 s.

3.4. Molecular weight of polymer

Three different molecular weights were chosen for PMMA-co-PtBA: 44000, 108500 and 285000 (see Table 1). The cross-section SEM images of the film heated at at 80 °C for 180 s are shown in Fig. 9. It is clearly seen that the cell size increases with the increase of molecular weight of PMMA-co-PtBA. Since the smaller M_w polymers have a lower viscosity (Fig. 10), it is speculated that they would not be able to capture a large amount of the gas bubbles in polymer matrix. When the M_w is sufficiently large, e.g., 285000, the polymer viscosity may become high enough to hold the gas bubbles in polymer matrix.

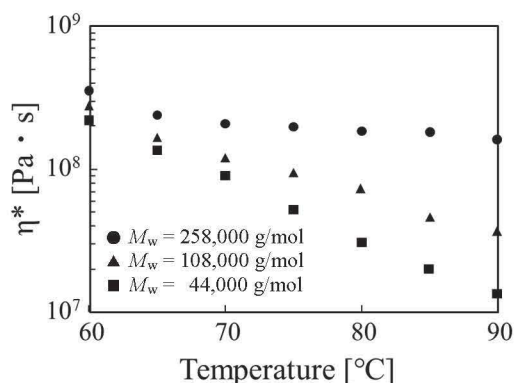


Fig. 10. Complex viscosity of PMMA-co-PtBA (η^*) as a function of temperature.

3.5. Comparison to physically foamed nanocellular structure

So far, by adjusting the process and materials parameters in the UV-induced chemical foaming, we were able to create the nanocellular foams with cell size and density ranging from ~100 to 200 nm and from $\sim 1 \times 10^{13}$ to 9×10^{13} cells/cm³, respectively. These specifications are comparable to those obtained from some physical foaming processes. For example, nanocellular structure generated by the heterogeneous nucleation process has cell size of ~200 to 600 nm and density of 10^{13} to 10^{14} cells/cm³ [18-22]. In this process, clay nanoparticles were added into some common polymer matrices, e.g., PLA, HDPE, PC and SAN, not only to induce heterogeneous nucleation but also to improve the mechanical strength of the foamed sample.

In case of physical foaming with block copolymer templates, the template was prepared by self-assembling the block copolymer into a periodic structure that consists of a CO₂-phallic domain. Then a supercritical CO₂ was injected to the self-

assembled block copolymer at a high pressure, followed by a rapid drop of the pressure. The final nanocellular foams had the cell size and density ranging from ~10 to 100 nm and from 10^{14} to 10^{16} cells/cm³, respectively [13,23,24]. It is expected that such cells may also be generated with the UV-induced chemical foaming method by further increasing the molecular weight of the polymer, the amount of PAG, and adjusting the PtBA ratio.

4. Conclusion

We have investigated a UV-induced chemical foaming process, where PMMA-co-PtBA was foamed by photoacid catalyzed deprotection of the *tert*-butyl ester group in PtBA. Using this method, nanocellular structures were generated with cell size and cell density ranging from 120 to 200 nm, and 4×10^{13} to 9×10^{13} cells/cm³, respectively.

By varying the foaming time, development of the nanocellular structure was observed. In the initial stage of foaming, small cells were sparsely formed throughout the film. With acceleration of the acid diffusion, the cell size and the cell density were gradually increased. After a certain foaming time, most of the *tert*-butyl ester group in PtBA was reacted and the gas generation was almost complete. At this stage, excess isobutene gas diffused out of the film, resulting in a slight decrease in cell size. Finally, the cell size and the cell density became unchanged.

We also demonstrated that the cell structure could be largely affected by the foaming temperature, UV irradiation and polymer molecular weight. For instance, the cell size and the cell density significantly increased with the increase of foaming temperature. This could be explained by the fact that the polymer was largely softened at higher temperatures. The polymer would also need a larger molecular weight to prevent the gas from diffusing out from the polymer matrix. As for the UV dose, a larger amount would be preferred since all PAG could be activated and therefore the cell nucleation sites could be increased.

References

1. C. Okolieocha, D. Raps, K. Subramaniam, and V. Altstädt, *Eur. Polym. J.*, **73** (2015) 500.
2. B. Notario, J. Pinto, E. Solonzano, J. de Saja, M. Dumon, and M. Rodríguez-Pérez, *Polymer*, **56** (2015) 57.
3. G. Wang, C. Wang, J. Zhao, G. Wang, C. Park, and G. Zhao, *Nanoscale*, **9** (2017) 5996.
4. S. S. Sundarram and W. Li, *Polym. Eng. Sci.*, **53** (2013) 1901.
5. B. Notario, J. Pinto, E. Solonzano, J. A. De Saja, M. Dumon, and M. A. Rodríguez-Pérez, *Polymer*, **56** (2015) 57.
6. S. K. Yeh, Y. C. Liu, C. C. Chu, K. C. Chang, and S. F. Wang, *Ind. Eng. Chem. Res.*, **56** (2017) 8499.
7. B. Notario, J. Pinto, and M. A. Rodríguez-Pérez, *Polymer*, **63** (2015) 116.
8. S. Costeus, *J. Appl. Polym. Sci.*, **131** (2014) 23.
9. C. B. Park, D. F. Baldwin, and N. P. Suh, *Polym. Eng. Sci.*, **35** (1995) 432.
10. Y. Ema, M. Ikeya, and M. Okamoto, *Polymer*, **47** (2006) 5350.
11. N. S. Ramesh and S. T. Lee, *Cell. Polym.*, **24** (2005) 269.
12. H. Yokoyama, L. Li, T. Nemoto, and K. Sugiyama, *Adv. Mater.*, **16** (2004) 1542.
13. H. Yokoyama and K. Sugiyama, *Macromolecules*, **38** (2005) 10516.
14. W. Michaeli and S. Sitz, *Cell. Polym.*, **29** (2010) 227.
15. N. Petchwattana and S. Covavisaruch, *Mater. Des.*, **32** (2011) 2844.
16. J. Kojima, T. Takada, and F. Jinno, *J. Cell. Plast.*, **43** (2007) 103.
17. L. Wang, Y. Hikima, M. Ohshima, and A. Yusa, *Chem. Eng. Sci.*, **61** (2006) 2108.
18. Y. Fujimoto, S. S. Ray, M. Okamoto, A. Ogami, K. Yamada, and K. Ueda, *Macromol. Rapid Commun.*, **24** (2003) 457.
19. H. Y. Lee, C. B. Park, K. H. Wang, and M. H. Lee, *J. Cell. Plast.*, **41** (2005) 487.
20. Y. Ito, M. Yamashita, and M. Okamoto, *Macromol. Mater. Eng.*, **291** (2006) 773.
21. L. Urbanczyk, C. Calberg, C. Detrembleur, C. Jerome, and M. Alexandre, *Polymer*, **51** (2010) 3520.
22. S. Costeux and L. Zhu, *Polymer*, **54** (2013) 2785.
23. K. Taki, Y. Waratani, and M. Ohshima, *Macromol. Mater. Eng.*, **293** (2008) 589.
24. J. A. Reglero Ruiz, M. Dumon, J. Pinto, and M. A. Rodríguez-Pérez, *Macromol. Mater. Eng.*, **296** (2011) 75.